Available online at www.sciencedirect.com
ScienceDirect
Ceramics International 36 (2010) 381–384
CERAMICS INTERNATIONAL
www.elsevier.com/locate/ceramint

Short communication

Mode I fracture toughness of SiC particle-dispersed ZrB_2 matrix composite measured using DCDC specimen

J.K. Kurihara [a], T. Tomimatsu [a], Y.F. Liu [a], S.Q. Guo [b], Y. Kagawa [a,b,*]

[a] *Research Center for Advanced Science and Technology, The University of Tokyo, 4-6-1, Komaba, Meguro-ku, Tokyo 153-8904, Japan*
[b] *National Institute for Materials Science, 1-2-1 Sengen, Tsukuba 305-0047, Japan*

Received 24 April 2009; received in revised form 3 June 2009; accepted 26 July 2009
Available online 25 August 2009

Abstract

Mode I fracture toughness of SiC particle-dispersed ZrB_2 matrix composite has been measured using DCDC specimen. Compression test results of the DCDC specimen show that the fracture toughness of the composite is independent of crack length with an average toughness $\sim 3.5\,\mathrm{MPa}\sqrt{m}$. Optical microscope and SEM observations reveal a flat crack path and fracture surface with no significant toughening mechanisms in the composite either through grain boundary deflection or SiC particle introduction. Comparison with previous ZrB_2 matrix composites, in addition to other short crack test methods, there is an agreement with the results between what this study has come upon with respect to previous work.
© 2009 Elsevier Ltd and Techna Group S.r.l. All rights reserved.

Keywords: Mechanical Properties; Fracture; ZrB_2; SiC particle; Composite

1. Introduction

ZrB_2 has recently received extensive attention due to its capabilities in ultrahigh temperatures [1,2], high thermal conductivity and electric conductivity [2–4]. These features are attractive for extremely high temperature applications, such as next generation aerospace structures [5,6]. Usually, SiC particles are added into ZrB_2 to increase sinterability [2,7,8], oxidation resistance [8,10,11] and thermal conductivity [4,8,12,13]. One poor property of SiC particle-dispersed ZrB_2 matrix composites (hereafter denotes as SiC/ZrB_2) is its low fracture toughness.

Reported fracture toughness measurements of SiC/ZrB_2 have been done through the Vickers indentation method [7,12–15] or bending of a notched bar specimen [9]. Because of the low fracture toughness in SiC/ZrB_2, Vickers indentation usually causes many sub-cracks to grow near the indenter edge and this behavior is sensitive to the applied load, making it difficult to define the growth of a unique pure mode I crack. In order to measure true fracture toughness of SiC/ZrB_2, it is desirable to obtain toughness under a well-controlled naturally grown crack. However, no experimental investigation has been performed to measure the toughness of SiC/ZrB_2 under a naturally grown sharp crack under a well-predicted phase angle at the crack tip.

It has been known that double cleavage-drilled compressive (DCDC) specimen gives close to mode I toughness under natural crack growth conditions. Therefore, using a DCDC specimen seems suitable to measure the mode I fracture toughness in SiC/ZrB_2. However, no experimental results are reported. The aim of this paper is to show mode I fracture toughness of SiC/ZrB_2 using a DCDC specimen.

2. Experimental procedure

α-SiC particle-dispersed ZrB_2 matrix composite plate was obtained from AGC Ceramics Co., Tokyo, Japan. The composite contains 10 vol% SiC and ∼4 vol% pores in the matrix and its typical microstructure is shown in Fig. 1. X-ray diffraction analysis confirms that the composite composed of α-SiC and ZrB_2. Observation of polished surfaces shows that the SiC particle distribution is randomly dispersed without noticeable segregations (Fig. 1).

The composite plate was cut into a double cleavage-drilled compressive (DCDC) specimen using a standard metallurgical cutting and polishing procedures. Final polishing, down to 0.5 μm diamond paste finish, of the surfaces was performed.

* Corresponding author. Tel.: +81 3 5452 5086; fax: +81 3 5452-5087.
E-mail address: kagawa@rcast.u-tokyo.ac.jp (Y. Kagawa).

0272-8842/$36.00 © 2009 Elsevier Ltd and Techna Group S.r.l. All rights reserved.
doi:10.1016/j.ceramint.2009.07.031

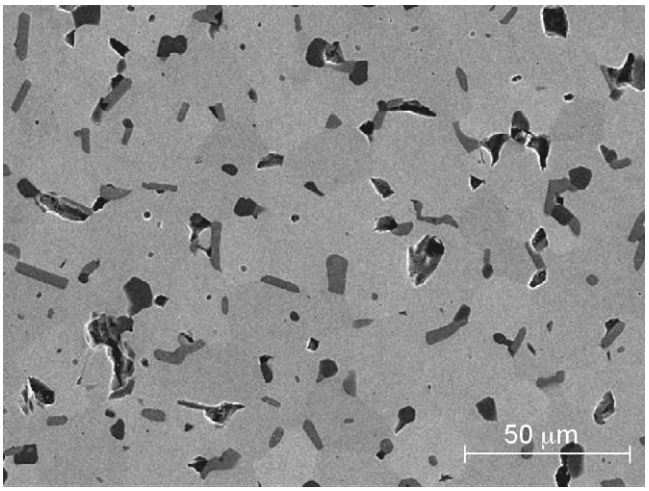

Fig. 1. Typical SEM micrograph of the ZrB_2–SiC material after polishing.

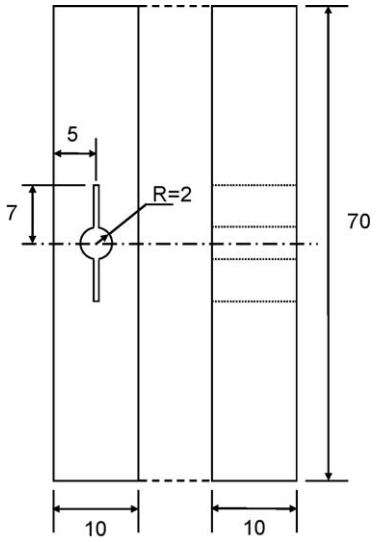

Fig. 2. Schematic of the DCDC specimen shape and dimensions in mm.

Fig. 2 shows shape and dimensions of the DCDC specimen. The specimen had length 70 mm ($2H$), thickness 10 mm ($2b$) and width 10 mm ($2w$). A through-thickness center hole with a diameter of 4 mm and starter notches were introduced by the arc discharge machining process. Starter notch width was 100 μm and a tip radius ∼50 μm.

Uniaxial compressive load was applied to the DCDC specimen to obtain stable crack propagation from notch tips. This specimen was chosen because conditions at the crack tip are very close to mode I [16]. A compressive load was applied to the DCDC specimen using a screw-type driven test machine (Instron Corp., Model 4204, NJ, USA). Tests were conducted in ambient air (20 °C) at a constant crosshead rate of 0.05 mm/s. During testing, loading was interrupted at a selected applied load and the specimen was removed from the machine to observe crack growth behavior by optical microscope and to measure crack lengths. The nominal resolution for measuring the crack length is less than 0.5 μm. Thereafter, the specimen was reloaded; this process was repeated until crack length extended from the notch ∼20 mm. This loading–unloading process did not affect crack growth behavior because it was confirmed that crack growth occurred only during the loading stage in the present work. After complete failure of the specimen, fracture surfaces were observed by scanning electron microscope (SEM).

3. Results and discussion

Stable crack growth is observed from both notch tips and the crack length increased with increasing applied load. Crack growth behavior from a notch tip is shown in Fig. 3. Near the notch root, the path shows large-scale wavy behavior and small

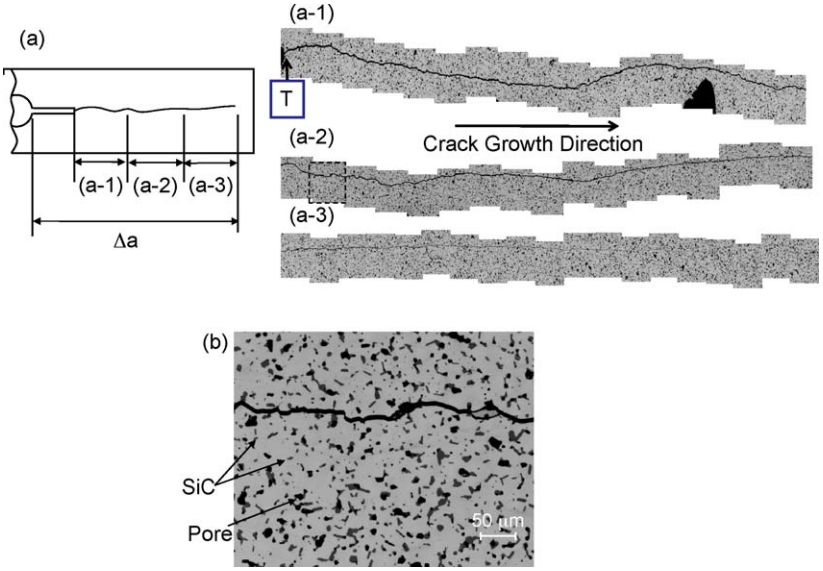

Fig. 3. Crack growth behavior from a notch tip shown in (a) the notch tip is signified by the [T]. The break up of (a) is through (a-1) to (a-3) and (b) shows the crack path magnified.

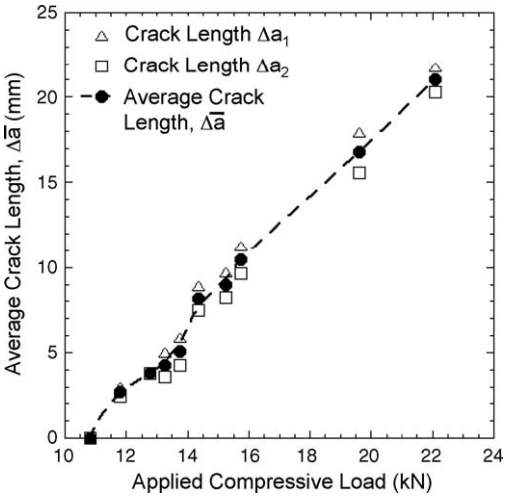

Fig. 4. An example of applied load versus crack lengths.

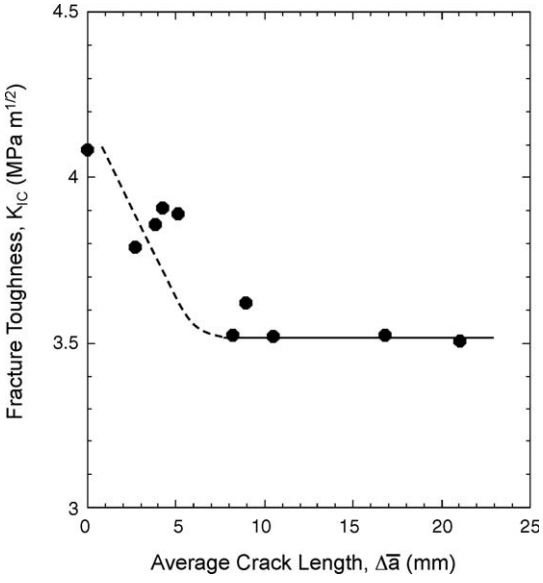

Fig. 5. Toughness versus the average crack length.

deflections are superimposed on it, thereafter, the path tends to become straight with increasing crack length. During test, both the crack lengths from a tip of initial notch, Δa_1 and Δa_2, are nearly equal within the maximum 16% difference, therefore, average value, $\Delta\bar{a}$, is used for calculation of the fracture toughness.

$$\Delta\bar{a} = \frac{1}{2}(\Delta a_1 + \Delta a_2). \tag{1}$$

Here, the crack length is defined as the shortest distance between initial crack tip and advancing crack tip drawn by lines parallel to loading direction, which is usually used for definition of crack length in a DCDC specimen [16–18].

Fig. 4 shows a typical example of the relation between applied load, P, versus crack lengths, $\Delta\bar{a}$. Plane strain fracture toughness of the SiC/ZrB_2 composite was obtained using the formula:

$$K_I(\Delta\bar{a}) = \sigma\sqrt{R}\left(F\left(\frac{\Delta\bar{a}}{R}, \frac{w}{R}\right)\right) \tag{2}$$

where σ is the applied compressive stress, $F(\Delta\bar{a}/R, w/R)$ is the non-dimensional function given by [17]:

$$F\left(\frac{\Delta\bar{a}}{R}, \frac{w}{R}\right) = \left(\frac{\sqrt{\pi}R}{w}\right)\left[1 + \left(\frac{\Delta\bar{a}}{R}\right)\left(0.235 - 0.259\frac{\Delta\bar{a}}{w}\right)\right]^{-1} \tag{3}$$

where R is the center hole radius and w is the width of specimen. In this case, $\Delta\bar{a}/R$ needs to be larger than about 2.5 for Eq. (2) to be applied [17].

Plots of fracture toughness, $K_I(\Delta\bar{a})$, versus average crack length, $\Delta\bar{a}$, are presented in Fig. 5. For the short-range cracks from 0 to 8 mm, Eq. (2) is not accurate; therefore the crack length range of $8.1 \leq \Delta\bar{a} \leq 21$ mm should be used and the toughness is in the range of $3.50 - 3.62\,\mathrm{MPa}\sqrt{m}$ with an average of $3.54\,\mathrm{MPa}\sqrt{m}$. Previous reports have shown fracture toughness of SiC/ZrB_2 to range from 3.5 to $6.1\,\mathrm{MPa}\sqrt{m}$ [19–21]. Addition of third particles, such as $ZrSi_2$, $MoSi_2$, ZrC, C, and YSZ [14,19–21], can increase the toughness.

Detailed observation of the fracture surface (Fig. 6) reveals small grain level crack deflection behavior, however, there are

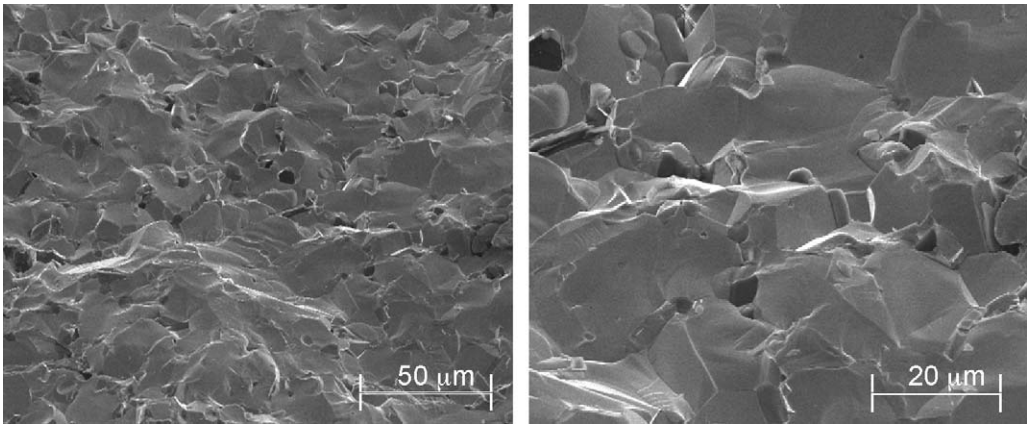

Fig. 6. SEM micrographs of the ZrB_2–SiC fracture surface.

several examples of cracking in the ZrB_2 that penetrates into SiC particles. From these observations, only slight crack deflection behavior contributes to toughening of SiC/ZrB_2, therefore the low fracture toughness of SiC/ZrB_2 originates from no useful effective toughening mechanisms in the composite.

4. Summary

Mode I fracture toughness of SiC particle-dispersed ZrB_2 matrix composite was measured using the DCDC specimen. The fracture toughness of the composite is $3.54\,\mathrm{MPa}\sqrt{m}$, independent of crack lengths. Only slight crack deflection behavior appears in the composite and almost no effective toughening mechanisms are involved in the composite.

References

[1] W.G. Fahrenholtz, G.E. Hilmas, Refractory diborides of zirconium and halfnium, J. Am. Ceram. Soc. 90 (5) (2007) 1347–1364.
[2] S.Q. Guo, Densification of ZrB_2-based composites and their mechanical and physical properties: a review, J. Eur. Ceram. Soc. 29 (2009) 995–1011.
[3] J.W. Zimmermann, G.E. Hilmas, W.G. Fahrenholtz, R.B. Dinwiddie, W.D. Porter, H. Wang, Thermophysical properties of ZrB_2 and ZrB_2–SiC ceramics, J. Am. Ceram. Soc. 91 (5) (2008) 1405–1411.
[4] S.Q. Guo, Y. Kagawa, T. Nishimura, H. Tanaka, Thermal and electrical properties in hot-pressed ZrB_2–$MoSi_2$–SiC composites, J. Am. Ceram. Soc. 90 (7) (2007) 2255–2258.
[5] K. Upadhya, J.-M. Yang, W.P. Hoffman, Materials for ultrahigh temperature structural applications, Am. Ceram. Soc. Bull. 76 (12) (1997) 51–56.
[6] F. Monteverde, A. Bellosi, L. Scatteia, Processing and properties of ultrahigh temperature ceramics for space applications, Mater. Sci. Eng. A 485 (2008) 415–421.
[7] S. Zhu, W.G. Fahrenholtz, G.E. Hilmas, Influence of silicon carbide particle size on the microstructure and mechanical properties of zirconium diboride–silicon carbide ceramics, J. Eur. Ceram. Soc. 27 (2007) 2077–2083.
[8] F. Monteverde, Beneficial effects of an ultra-fine a-SiC incorporation on the sinterability and mechanical properties of ZrB_2, Appl. Phys. A 82 (2006) 329–337.
[9] A. Rezaie, W.G. Fahrenholtz, G.E. Hilmas, Effect of hot pressing time and temperature on the microstructure and mechanical properties of ZrB_2–SiC, J. Mater. Sci. 42 (2007) 2735–2744.
[10] W. Han, X. Zhang, J. Han, S. Meng, High-temperature oxidation at 1900 °C of ZrB_2–xSiC ultrahigh-temperature ceramic composites, J. Am. Ceram. Soc. 91 (10) (2008) 3328–3334.
[11] F. Peng, R.F. Speyer, Oxidation resistance of fully dense ZrB_2 with SiC, TaB_2, and $TaSi_2$ additives, J. Am. Ceram. Soc. 91 (5) (2008) 1489–1494.
[12] W. Tian, Y. Kan, G. Zhang, P. Wang, Effect of carbon nanotubes of the properties of ZrB_2–SiC ceramics, Mater. Sci. Eng. A 287 (2008) 568–573.
[13] S.Q. Guo, Y. Kagawa, T. Nishimura, D. Ching, J. Yang, Mechanical and physical behavior of spark plasma sintered ZrC–ZrB_2–SiC composites, J. Eur. Ceram. Soc. 28 (2008) 1279–1285.
[14] W. Li, X. Zhang, C. Hong, W. Han, Hot-pressed ZrB_2–SiC–YSZ composites with various yttria content: microstructure and mechanical properties, Mater. Sci. Eng. A 494 (2008) 47–152.
[15] S. Zhang, G.E. Hilmas, W.G. Fahrenholtz, Pressureless sintering of ZrB_2–SiC ceramics, J. Am. Ceram. Soc. 91 (1) (2008) 26–32.
[16] M.R. Turner, B.J. Dalgleish, M.Y. He, A.G. Evans, A fracture resistance measurement method for biomaterial interfaces having large Debond energy, Acta Met. Mater. 43 (9) (1995) 3459–3465.
[17] M. Hasegawa, S.J. Zhu, Y. Kagawa, A.G. Evans, Effect of metal layer thickness on the decohesion of high purity copper–saphire interfaces, Acta Mater. 51 (2003) 5113–5121.
[18] C.G. Sammis, M.F. Ashby, The failure of brittle porous solids under compressive stress states, Acta Metall. 34 (3) (1986) 511–526.
[19] A. Bellosi, F. Monteverde, D. Sciti, Fact densification of ultra-high-temperature ceramics by spark plasma sintering, Int. J. Appl. Ceram. Technol. 3 (1) (2006) 32–40.
[20] S.Q. Guo, Y. Kagawa, T. Nishimura, H. Tanaka, Pressureless sintering and physical properties of ZrB_2-based composites with $ZrSi_2$ additive, Scripta Mater. 58 (2008) 579–582.
[21] W. Guo, X. Zhou, G. Zhang, Y. Kan, Y. Li, P. Wang, Effect of Si addition on hot-pressed ZrB_2–SiC composite with polycarbosilane as a precursor, Mater. Lett. 62 (2008) 3724–3726.